

Topological Phase Transition and Electrically Tunable Diamagnetism in Silicene

Motohiko Ezawa

Department of Applied Physics, University of Tokyo, Hongo 7-3-1, 113-8656, Japan

Silicene is a monolayer of silicon atoms forming a honeycomb lattice. The lattice is actually made of two sublattices with a tiny separation. Silicene is a topological insulator, which is characterized by a full insulating gap in the bulk and helical gapless edges. It undergoes a phase transition from a topological insulator to a band insulator by applying external electric field. Analyzing the spin Chern number based on the effective Dirac theory, we find their origin to be a pseudospin meron in the momentum space. The pseudospin degree of freedom arises from the two-sublattice structure. Our analysis makes clear the mechanism how a phase transition occurs from a topological insulator to a band insulator under increasing electric field. We propose a method to determine the critical electric field with the aid of diamagnetism of silicene. Diamagnetism is tunable by the external electric field, and exhibits a singular behaviour at the critical electric field. Our result is important also from the viewpoint of cross correlation between electric field and magnetism. Our finding will be important for future electro-magnetic correlated devices.

INTRODUCTION

Silicene has recently been synthesized[1–4] and attracted much attention[5–7]. It is a monolayer of silicon atoms forming a two-dimensional honeycomb lattice. Almost every striking property of graphene could be transferred to this innovative material. Indeed, its low-energy dynamics is described by the Dirac theory as in graphene. However, Dirac electrons are massive due to a relatively large spin-orbit (SO) gap of 1.55meV in silicene, where the mass can be controlled by applying the electric field E_z perpendicular to the silicene sheet[6]. A novel feature is that silicene is a topological insulator[5], which is characterized by a full insulating gap in the bulk and helical gapless edges.

Silicene undergoes a topological phase transition from a topological insulator to a band insulator as $|E_z|$ increases and crosses the critical field E_{cr} , as has been shown[6] by examining numerically the emergence of the helical zero energy modes in silicene nanoribbons. In this paper we present an analytic result by calculating the topological numbers based on the effective Dirac theory. We show that the origin of the topological numbers is a pseudospin meron in the momentum space. The pseudospin degree of freedom arises from the two-sublattice structure (Fig.1). We also propose a simple method to determine experimentally the phase transition point with the use of the diamagnetism of silicene (Fig.1).

The magnetism of conventional metal is composed of the Pauli paramagnetism due to the spin magnetic moment and the Landau diamagnetism due to the orbital motion of electrons. The free electron system exhibits paramagnetism since the magnitude of the spin component is larger than the orbital component. Contrarily, the Landau diamagnetism overcomes the Pauli paramagnetism in a certain condensed matter system. An extreme case is provided by graphene[8–12], where the orbital susceptibility has a strong singularity due to the gapless character of Dirac electrons.

We calculate the magnetic susceptibility of silicene as a function of the electric field E_z . We expect to have a strong singularity at the critical electric field, $|E_z| = E_{cr}$, since Dirac electrons become gapless at this point[6]. Indeed, we

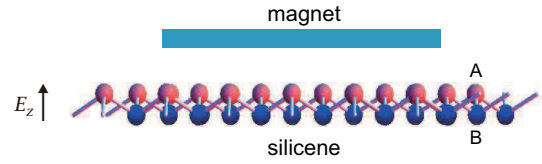


FIG. 1: (Color online) Illustration of an experimental setting to determine the critical electric field E_{cr} with the use of the magnetic susceptibility of silicene. Silicene consists of a honeycomb lattice of silicon atoms with two sublattices made of A sites (red) and B sites (blue). The two sublattice planes are separated by a distance. A strong diamagnetism emerges between a magnet and a silicene sheet at the topological phase transition point $E_z = E_{cr}$.

show that it diverges at the critical electric field at zero temperature ($T = 0$), though the divergence is round off at finite temperature. However, it is clearly observable as long as $k_B T \lesssim \frac{1}{10} \lambda_{SO}$. Our result is important also from the viewpoint of cross correlation between electric field and magnetism. In general electric-field-controlled magnetism is rather difficult compared to magnetic-field-controlled electricity. On the other hand, the former is desirable since we can precisely control electric field. Our finding will be important for future electro-magnetic correlated devices.

TIGHT BINDING MODEL

Silicene consists of a honeycomb lattice of silicon atoms with two sublattices made of A sites and B sites. The two sublattices are separated by a distance, which we denote by 2ℓ with $\ell = 0.23\text{\AA}$. The silicene system is described by the four-band second-nearest-neighbor tight binding model[6, 13, 14],

$$H_0 = -t \sum_{\langle i,j \rangle \alpha} c_{i\alpha}^\dagger c_{j\alpha} + i \frac{\lambda_{SO}}{3\sqrt{3}} \sum_{\langle\langle i,j \rangle\rangle \alpha\beta} \nu_{ij} c_{i\alpha}^\dagger \sigma_{\alpha\beta}^z c_{j\beta} - i \frac{2}{3} \lambda_{R2} \sum_{\langle\langle i,j \rangle\rangle \alpha\beta} \mu_i c_{i\alpha}^\dagger \left(\boldsymbol{\sigma} \times \hat{\mathbf{d}}_{ij} \right)_{\alpha\beta}^z c_{j\beta}, \quad (1)$$

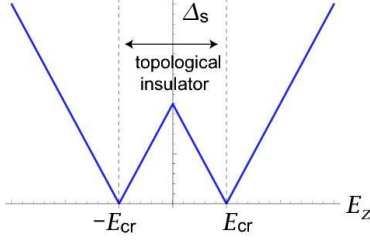


FIG. 2: The band gap Δ_s as a function of the electric field E_z . The gap is open for $E_z \neq \pm E_{cr}$, where silicene is an insulator. It has been shown[6] that it is a topological insulator for $|E_z| < E_{cr}$ and a band insulator $|E_z| > E_{cr}$. Thus there occurs a topological phase transition at $|E_z| = E_{cr}$.

where $c_{i\alpha}^\dagger$ creates an electron with spin polarization α at site i , and $\langle i, j \rangle / \langle\langle i, j \rangle\rangle$ run over all the nearest/next-nearest neighbor hopping sites. The first term represents the usual nearest-neighbor hopping with the transfer energy $t = 1.6\text{eV}$. The second term represents the effective SO coupling with $\lambda_{SO} = 3.9\text{meV}$, where $\sigma = (\sigma_x, \sigma_y, \sigma_z)$ is the Pauli matrix of spin, with $\nu_{ij} = +1$ if the next-nearest-neighboring hopping is anticlockwise and $\nu_{ij} = -1$ if it is clockwise with respect to the positive z axis. The third term represents the second Rashba SO coupling with $\lambda_{R2} = 0.7\text{meV}$ associated with the next-nearest neighbor hopping term, where $\mu_i = \pm 1$ for the A (B) site, and $\hat{d}_{ij} = \mathbf{d}_{ij}/|\mathbf{d}_{ij}|$ with the vector \mathbf{d}_{ij} connecting two sites i and j in the same sublattice.

We take a silicene sheet on the xy -plane, and apply the electric field E_z perpendicular to the plane. There appear two additional terms in the Hamiltonian,

$$H_E = i\lambda_{R1}(E_z) \sum_{\langle i, j \rangle \alpha \beta} c_{i\alpha}^\dagger \left(\boldsymbol{\sigma} \times \hat{\mathbf{d}}_{ij} \right)_{\alpha\beta}^z c_{j\beta} + \ell \sum_{i\alpha} \mu_i E_z c_{i\alpha}^\dagger c_{i\alpha}, \quad (2)$$

where the first term represents the first Rashba SO coupling associated with the nearest neighbor hopping, which is induced by external electric field[15, 16]. It is proportional to the external electric field, $\lambda_{R1}(E_z) \propto E_z$, and becomes of the order of $10\mu\text{eV}$ at $E_z = \lambda_{SO}/\ell = 17\text{meV}\text{\AA}^{-1}$. The second term is the staggered sublattice potential term $\propto 2\ell E_z$ between silicon atoms at A sites and B sites. The total Hamiltonian is given by $H = H_0 + H_E$. We note that the first Rashba SO coupling term ($\propto \lambda_{R1}$) is missed in the previous analysis[6].

DIRAC THEORY

Electronic states near the Fermi energy are π orbitals residing near the K and K' points at opposite corners of the hexagonal Brillouin zone. We also call them the K_η points with $\eta = \pm$. The low-energy effective Hamiltonian is derived from the tight binding model $H = H_0 + H_E$. It is described by the

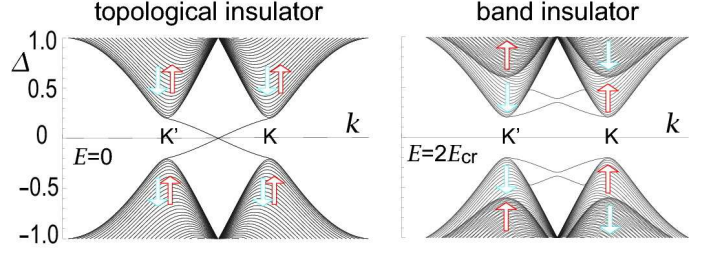


FIG. 3: (Color online) One-dimensional energy bands for a silicene nanoribbon. (a) The bands crossing the gap represent edge states, demonstrating that it is a topological insulator. (b) All states are gapped, demonstrating that it is a band insulator.

Dirac theory around the K_η point as

$$H_\eta = \hbar v_F (\eta k_x \tau_x + k_y \tau_y) + \eta \tau_z h_{11} + \ell E_z \tau_z + \lambda_{R1} (\eta \tau_x \sigma_y - \tau_y \sigma_x) / 2 \quad (3)$$

with

$$h_{11} = \lambda_{SO} \sigma_z + a \lambda_{R2} (k_y \sigma_x - k_x \sigma_y), \quad (4)$$

where τ_a is the Pauli matrix of the sublattice pseudospin, $v_F = \frac{\sqrt{3}}{2}at$ is the Fermi velocity, and $a = 3.86\text{\AA}$ is the lattice constant.

The band gap is located at the K and K' points. At these points the energy is exactly given by

$$\mathcal{E}_s = \lambda_{SO} + s\ell E_z, \quad \lambda_{SO} + s\sqrt{(\ell E_z)^2 + \lambda_{R1}^2} \quad (5)$$

where $s = \pm 1$ is the spin-chirality. It is given by $s = s_z \eta$ when the spin s_z is a good quantum number. The gap is given by $2|\Delta_s(E_z)|$ with

$$\Delta_s(E_z) = -s\lambda_{SO} + \frac{1}{2}\ell E_z + \frac{1}{2}\sqrt{(\ell E_z)^2 + \lambda_{R1}^2}. \quad (6)$$

As $|E_z|$ increases, the gap decreases linearly since $\lambda_{R1} \propto E_z$, and vanishes at the critical point $|E_z| = E_{cr}$ with

$$E_{cr} = \frac{s\lambda_{SO}}{\ell} \left[1 - \left(\frac{\lambda_{R1}}{2\lambda_{SO}} \right)^2 \right] = \pm 17\text{meV}/\text{\AA}, \quad (7)$$

and then increases linearly (Fig.2) The correction due to the first Rashba coupling is extremely small, $(\lambda_{R1}/2\lambda_{SO})^2 = 10^{-4}$.

SPIN CHERN NUMBER

We have shown in a previous paper[6] that silicene is a topological insulator for $|E_z| < E_{cr}$ and it is a band insulator for $|E_z| > E_{cr}$ by examining numerically the emergence of the helical zero energy modes in a silicene nanoribbon (Fig.3). In this section we present an analytic discussion by calculating the topological numbers based on the effective Dirac theory.

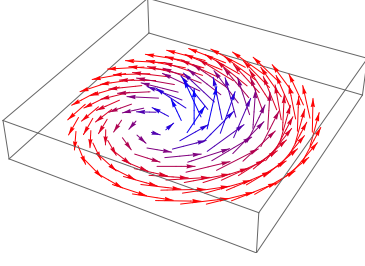


FIG. 4: Illustration of a meron in momentum space. The pseudospin texture is a meron for each spin in each valley, which yields $1/2$ to the Pontryagin number.

The topological quantum numbers are the Chern number \mathcal{C} and the \mathbb{Z}_2 index. If the spin s_z is a good quantum number, the \mathbb{Z}_2 index is identical to the spin-Chern number \mathcal{C}_s modulo 2. They are defined when the state is gapped, and given by

$$\mathcal{C} = \mathcal{C}_+ + \mathcal{C}_-, \quad \mathcal{C}_s = \frac{1}{2}(\mathcal{C}_+ - \mathcal{C}_-), \quad (8)$$

where \mathcal{C}_\pm is the summation of the Berry curvature in the momentum space over all occupied states of electrons with $s_z = \pm 1$. They are well defined even if the spin is not a good quantum number[17, 18]. In the present model the spin is not a good quantum number because of spin mixing due to the Rashba couplings λ_{R1} and λ_{R2} , and the resulting angular momentum eigenstates are indexed by the spin chirality $s = \pm 1$. A convenient way of calculating the Chern number \mathcal{C} and the \mathbb{Z}_2 index is to use the formula (8) to the system without the Rashba couplings and then adiabatically switching on these couplings to recover the present system[17, 18].

When we set $\lambda_{R1} = 0$ and $\lambda_{R2} = 0$, the Hamiltonian (3) becomes block diagonal. For each spin $s_z = \pm 1$ and valley $\eta = \pm 1$, it describes a two-band system in the form,

$$H = \boldsymbol{\tau} \cdot \mathbf{d}, \quad (9)$$

where

$$d_x = \eta \hbar v_F k_x, \quad d_y = \hbar v_F k_y, \quad d_z = m_D, \quad (10)$$

with the Dirac mass

$$m_D = s\lambda_{SO} + \ell E_z. \quad (11)$$

The summation of the Berry curvature is reduced to the Pontryagin index in the two-band system[19],

$$\mathcal{C}_{s_z}^\eta = \frac{1}{4\pi} \int d^2k \left(\frac{\partial \hat{\mathbf{d}}}{\partial k_x} \times \frac{\partial \hat{\mathbf{d}}}{\partial k_y} \right) \cdot \hat{\mathbf{d}} \quad (12)$$

where $\hat{\mathbf{d}} = \mathbf{d}/|\mathbf{d}|$ is the unit vector which specifies the direction of \mathbf{d} . It is equal to the number of times the unit sphere is covered upon integrating over the Brillouin zone.

It is convenient to use the cylindrical coordinate in the momentum space, where

$$\hat{d}_x \pm i\hat{d}_y = \sqrt{1 - \sigma^2(k)} e^{i\eta\theta}, \quad \hat{d}_z = \sigma(k) \quad (13)$$

with

$$\sigma(k) = \frac{m_D}{\sqrt{(\hbar v_F k)^2 + m_D^2}}, \quad (14)$$

The pseudospin texture (13) describes a vortex-like meron in the momentum space, as shown in Fig.4. The Pontryagin index (12) yields

$$\mathcal{C}_{s_z}^\eta = \frac{\eta}{4\pi} \int d^2k \varepsilon_{ij} \partial_i \sigma \partial_j \theta = \frac{\eta}{2} \text{sgn}(m_D) \int_0^1 d\sigma.$$

Hence we find

$$\mathcal{C} = \sum_{\eta=\pm} (\mathcal{C}_+^\eta + \mathcal{C}_-^\eta) = 0, \quad (15)$$

$$\mathcal{C}_s = \sum_{\eta=\pm} \frac{1}{2} (\mathcal{C}_+^\eta - \mathcal{C}_-^\eta) = \Theta(\lambda_{SO} - \ell|E_z|), \quad (16)$$

where Θ is the step function, i.e.,

$$\mathcal{C}_s = \begin{cases} 1 & \text{for } |\ell E_z| < \lambda_{SO} \\ 0 & \text{for } |\ell E_z| > \lambda_{SO} \end{cases}. \quad (17)$$

We have verified that the system is a topological insulator for $|\ell E_z| < \lambda_{SO}$ and a band insulator for $|\ell E_z| > \lambda_{SO}$ in the system without the Rashba interactions. The property remains true when they are switched on adiabatically.

DIAMAGNETISM

We proceed to discuss a possible experimental method to detect the phase transition point by measuring the magnetic susceptibility. We apply homogeneous magnetic field $\mathbf{B} = \nabla \times \mathbf{A} = (0, 0, -B)$ with $B > 0$ along the z axis to silicene[7]. By making the minimal substitution, the Hamiltonian is given by

$$H_\eta = v_F (\eta P_x \tau_x + P_y \tau_y) + \eta \tau_z \hbar_{11} + \ell E_z \tau_z + \lambda_{R1} (\eta \tau_x \sigma_y - \tau_y \sigma_x) / 2 \quad (18)$$

with the covariant momentum $P_i \equiv \hbar k_i + eA_i$. We introduce a pair of Landau-level ladder operators,

$$\hat{a} = \frac{\ell_B (P_x + iP_y)}{\sqrt{2}\hbar}, \quad \hat{a}^\dagger = \frac{\ell_B (P_x - iP_y)}{\sqrt{2}\hbar}, \quad (19)$$

satisfying $[\hat{a}, \hat{a}^\dagger] = 1$, where $\ell_B = \sqrt{\hbar/eB}$ is the magnetic length. In the basis $\{\psi_{A\uparrow}, \psi_{B\uparrow}, \psi_{A\downarrow}, \psi_{B\downarrow}\}^t$, the Hamiltonian H_+ reads

$$\begin{pmatrix} \Delta_+^0(E_z) & \hbar\omega_c \hat{a}^\dagger & i\frac{\sqrt{2}\hbar a \lambda_{R2}}{\ell_B} \hat{a}^\dagger & 0 \\ \hbar\omega_c \hat{a} & -\Delta_+^0(E_z) & -i\lambda_{R1} & -i\frac{\sqrt{2}\hbar a \lambda_{R2}}{\ell_B} \hat{a}^\dagger \\ -i\frac{\sqrt{2}\hbar a \lambda_{R2}}{\ell_B} \hat{a} & i\lambda_{R1} & \Delta_-^0(E_z) & \hbar\omega_c \hat{a}^\dagger \\ 0 & i\frac{\sqrt{2}\hbar a \lambda_{R2}}{\ell_B} \hat{a} & \hbar\omega_c \hat{a} & -\Delta_-^0(E_z) \end{pmatrix}, \quad (20)$$

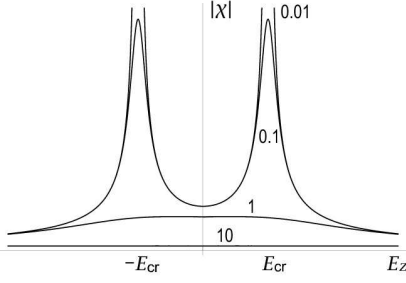


FIG. 5: Susceptibility χ as a function of electric field E_z for various temperature $k_B T / \lambda_{SO} = 0.01, 0.1, 1, 10$. It has a sharp peak at $|E_z| = E_{cr}$ for $k_B T / \lambda_{SO} \lesssim 0.1$, and diverges as $T \rightarrow 0$.

at the K point, with $\omega_c = \sqrt{2}\hbar v_F / \ell_B$. Here the diagonal elements $\Delta_{\pm}^0(E_z)$ are

$$\Delta_{\pm}^0(E_z) = \pm \lambda_{SO} + \ell E_z t_z \quad (21)$$

with the sublattice pseudospin t_z . We note that $\Delta_{\pm}(E_z) = \Delta_{\pm}^0(E_z)$ if we set $\lambda_{R1} = 0$.

The magnetic susceptibility is defined by

$$\chi = \lim_{B \rightarrow 0} \frac{M}{B}, \quad (22)$$

where M is the magnetization and B is the external magnetic field. The general formula for the orbital magnetic susceptibility of Bloch electrons is given by[20],

$$\chi = -g_v \frac{e^2 \hbar^2 v_F^2}{6\beta \pi c^2} \sum_n \sum_k \text{Tr}(G v_x G v_y G v_x G v_y), \quad (23)$$

where $v_i = \partial H / \partial k_i$, $\beta = 1/k_B T$, and G is the temperature Green function

$$G(k, \omega_n) = (i\hbar\omega_n - H)^{-1}, \quad (24)$$

with $\hbar\omega_n = (2n + 1)\pi/\beta$ being the Matsubara frequency.

By making the Taylor expansion of (23) with respect to λ_{R1} and λ_{R2} , the Rashba terms are found to yield second order corrections, $\delta\chi = o(\lambda_{R1}^2/\hbar^2 v_F^2) + o(\lambda_{R2}^2/\hbar^2 v_F^2)$, and hence we neglect the Rashba terms in what follows. In this approximation the spin s_z is a good quantum number.

Integrating out the wave number k of the matrix trace of (23), we have

$$\sum_k \text{Tr}(G v_x G v_y G v_x G v_y) = \sum_{s=\pm} \frac{2}{\hbar^2 \omega_n^2 + \Delta_s^2}. \quad (25)$$

Using the formula of the infinite sum,

$$\sum_n \frac{1}{\hbar^2 \omega_n^2 + \Delta_s^2} = \frac{1}{2\Delta_s k_B T} \tanh \frac{\Delta_s}{2k_B T}, \quad (26)$$

we obtain the magnetic susceptibility at finite temperature,

$$\chi(T, E_z) = -g_v \frac{e^2 \hbar^2 v_F^2}{6\pi c^2} \sum_{s=\pm} \frac{1}{\Delta_s} \tanh \frac{\Delta_s}{k_B T}. \quad (27)$$

where $g_v = 2$ represents the valley degree of freedom. We show $\chi(T, E_z)$ as a function of E_z for typical values of T .

We can make a precise determination of the critical electric field E_{cr} based on this formula. Let us consider, for example, a situation where a magnet is placed parallel to a silicene sheet (Fig.1). The magnetization of silicene is given by $M = -|\chi|B$, where B is the external magnetic field made by the magnet. The magnet feels a strong repulsive force at $E_z = E_{cr}$, since we have $\Delta_s \rightarrow 0$ and $M \rightarrow -\infty$ as $|E_z| \rightarrow E_{cr}$ at $T = 0$. Even for finite temperature, $\chi(T, E_z)$ has a sharp peak at $|E_z| = E_{cr}$ for $k_B T \lesssim \lambda_{SO}/10$ as in Fig.5. Such a strong repulsive force can be detected mechanically.

I am very much grateful to N. Nagaosa for many fruitful discussions on the subject. This work was supported in part by Grants-in-Aid for Scientific Research from the Ministry of Education, Science, Sports and Culture No. 22740196.

-
- [1] B. Lalmi, H. Oughaddou, H. Enriquez, A. Kara, S. Vizzini, B. Ealet, and B. Aufray, Appl. Phys. Lett. **97**, 223109 (2010).
 - [2] P.E. Padova, C. Quaresima, C. Ottaviani, P.M. Sheverdyaeva, P. Moras, C. Carbone, D. Topwal, B. Olivieri, A. Kara, H. Oughaddou, B. Aufray, and G.L. Lay, Appl. Phys. Lett. **96**, 261905 (2010).
 - [3] B. Aufray A. Vizzini, H. Oughaddou, C. Lndri, B. Ealet, and G.L. Lay, Appl. Phys. Lett. **96**, 183102 (2010).
 - [4] P. Vogt, , P. De Padova, C. Quaresima, J. A., E. Frantzeskakis, M. C. Asensio, A. Resta, B. Ealet and G. L. Lay, Phys. Rev. Lett. **108**, 155501 (2012).
 - [5] C.-C. Liu, W. Feng, and Y. Yao, Phys. Rev. Lett. **107**, 076802 (2011).
 - [6] M. Ezawa, New J. Phys. **14**, 033003 (2012).
 - [7] M. Ezawa, J. Phys. Soc. Jpn. **81**, 064705 (2012).
 - [8] J. W. McClure, Phys. Rev. **104**, 666 (1956); J. W. McClure, Phys. Rev. **119**, 606 (1960).
 - [9] M. Koshino, Y. Arimura and T. Ando, Phys. Rev. Lett. **102**, 177203 (2009).
 - [10] M. Koshino and T. Ando, Phys. Rev. B **81**, 195431 (2010).
 - [11] M. Nakamura, Phys. Rev. B **76**, 113301 (2007).
 - [12] Y. Arimura and T. Ando, J. Phys. Soc. Jpn. **81**, 024702 (2012).
 - [13] C. L. Kane and E. J. Mele, Phys. Rev. Lett. **95**, 226801 (2005).
 - [14] C.-C. Liu, H. Jiang, and Y. Yao, Phys. Rev. B, **84**, 195430 (2011).
 - [15] H. Min, J. E. Hill, N. A. Sinitsyn, B. R. Sahu, L. Kleinman, and A. H. MacDonald, Phys. Rev. B **74**, 165310 (2006).
 - [16] W.K. Tse Z. Qiao, Y. Yao, A. H. MacDonald, and Qian Niu, Phys. Rev. B **83**, 155447 (2011).
 - [17] E. Prodan, Phys. Rev. B **80**, 125327 (2009).
 - [18] Y. Yang, Z. Xu, L. Sheng, B. Wang, D.Y. Xing, and D. N. Sheng, Phys. Rev. Lett. **107**, 066602 (2011).
 - [19] X.-L. Qi and S.-C. Zhang, Rev. Mod. Phys. **83**, 1057 (2011).
 - [20] H. Fukuyama, Prog. Theor. Phys., **45** 704 (1971).